Exp Brain Res (1981) 44: 213–228

Experimental Brain Research

Magnification Factor and Receptive Field Size in Foveal Striate Cortex of the Monkey* **

B.M. Dow, A.Z. Snyder, R.G. Vautin, and R. Bauer

Division of Neurobiology, Department of Physiology, School of Medicine, State University of New York, Buffalo, NY 14226, USA

Summary. Receptive field size and magnification have been studied in striate cortex of awake, behaving rhesus monkeys at visual eccentricities in the range of 5–160 min. The major findings that emerge are (1) magnification in the foveola achieves values in the range of 30 mm/deg, (2) mean field size is not proportional to inverse magnification in contrast with previous reports, and (3) the product, magnification × aggregate field size, is greater in central vision than in peripheral vision. Thus, a point of light projected onto foveal retina is "seen" by larger numbers of striate cortical cells than a point of light projected onto peripheral retina.

Implications of these findings for visual localization and two-point discrimination are discussed.

Key words: Striate cortex – Monkey – Magnification – Fovea – Receptive field – Visual acuity

The presence of a systematic topographic map of the visual field onto the monkey's striate cortex was first reported by Talbot and Marshall (1941) and subsequently confirmed by Daniel and Whitteridge (1961) on the basis of multi-unit recordings. Daniel and Whitteridge (1961) coined the term "magnification factor" to describe the amount of cortical surface devoted to a given portion of visual space. Their plot of magnification factor (in mm/deg) as a function of eccentricity demonstrated the greatly expanded foveal representation in striate cortex.

Daniel and Whitteridge (1961) concluded that magnification factor in the foveal region of striate cortex achieved a maximum of about 6 mm/deg. Since central visual acuity (minimal angle of resolution) for macaque monkeys was known to be about 0.67′ (Grether 1941), the cortical projection of central visual acuity was, therefore, a distance of 67 μm (0.67 min × 6 mm/deg × $\frac{1}{60}\frac{\text{deg}}{\text{min}}$ × 1,000 $\frac{\mu\text{m}}{\text{mm}}$). Daniel and Whitteridge plotted inverse magnification (M^{-1}) against eccentricity and compared this with Wertheim's (1894) earlier plot of human minimal angle of resolution against eccentricity. Since the two curves appeared to be parallel over an eccentricity range of 1°–70°, Daniel and Whitteridge (1961) asserted that a cortical distance of 67 μm corresponded to the minimum angle of resolution at all eccentricities. They proposed a model for cortical acuity, according to which two peaks of excitation in the cortex would have to be separated by the acuity distance in order for the activating stimuli to be recognized perceptually as separate points.

Since minimal angle of resolution closely approximates cone size at eccentrictities of 5° or less (LeGrand 1967), Daniel and Whitteridge's (1961) postulated acuity distance of 67 μm should be equivalent at these eccentricities to cone separation plotted onto the cortex. Daniel and Whitteridge's (1961) acuity model, based on two just resolvable peaks of cortical activity, thus amounted to a presumption, for central vision, that cortical receptive fields would be about the size of single cones. Polyak's (1957) "midget system", carrying foveal cone input into the brain by private channels, likewise postulated cone-sized cortical receptive fields in foveal striate cortex.

Hubel and Wiesel (1974) conducted a later mapping experiment involving measurements at seven eccentricities in the striate cortex of macaque monkeys. Using microelectrodes to record single units, Hubel and Wiesel (1974) examined both receptive field size and inverse magnification as functions of eccentricity. They found the two curves to be parallel straight lines over a range of 1°–22°. (Daniel and

* Dedicated to Hermann Rahn

** Supported by NIH grants EY02349 and 5 T32 EY07019

Offprint requests to: Dr. B.M. Dow, Neurobiology Laboratories, SUNY/Buffalo, 4234 Ridge Lea Road, Amherst, NY 14226, USA

0014–4819/81/0044/0213/$ 3.20

Whitteridge's [1961] M^{-1} curve was in fact not a straight line.) Hubel and Wiesel (1974) concluded that the aggregate receptive field (mean field size plus scatter) at a given recording site was just large enough that a 2–3 mm cortical displacement in any direction would yield completely new receptive fields having no overlap with the old ones. They commented that this was about the same as "hypercolumn" size (Hubel and Wiesel 1974), a hypercolumn consisting of a pair of ocular dominance columns or a complete set of orientation columns. In fact, 2–3 mm is two or three times hypercolumn size, as they recognized. Later they reduced their estimate of the nonoverlap distance to 1–2 mm (Hubel and Wiesel 1977).

Hubel and Wiesel's receptive field nonoverlap distance, the cortical projection of the boundaries of an average cortical receptive field plus scatter, is equivalent to a cortical "point image" (see McIlwain 1976), the distribution of cortical neural activity resulting from a point of light on the retina. If we take 2 mm as the best estimate of Hubel and Wiesel's (1974) nonoverlap distance, the implication of their paper is that point image size is about 2 mm at all eccentricities between 1° and 22° in monkey striate cortex.

Now, a distance of 2 mm corresponds to almost 30× Daniel and Whitteridge's (1961) acuity distance. Converting to visual fields coordinates, this amounts to a ratio of 30:1 between cortical aggregate field size and minimal angle of resolution. Clearly Hubel and Wiesel's (1974) aggregate fields were much too large to support the earlier notions of MAR-sized or cone-sized cortical aggregate fields. However, Hubel and Wiesel's 2 mm point image was based on mean receptive field size. The possibility still existed that two-point discrimination might be dependent on a subpopulation of striate cortical cells with receptive fields as small as minimal angle of resolution or cone separation.

Over the past several years our laboratory has been examining response properties of single cells in striate cortex of monkeys performing a visual fixation task. In the course of these experiments it has been possible to obtain receptive field maps for large numbers of cells at known eccentricities in the range of 5 min to 2 degrees, thus permitting the earlier mapping studies of Talbot and Marshall (1941), Daniel and Whitteridge (1961), and Hubel and Wiesel (1974) to be extended toward zero eccentricity. Technical considerations have not permitted us to examine receptive fields at eccentricities of less than 5 min. Our main finding is that inverse magnification decreases at a much greater rate with decreasing eccentricity than does either receptive field size or minimal angle of resolution. Neither acuity distance nor point image size is invariant with eccentricity, though their ratio remains fixed at about 30:1.

Methods

Rhesus monkeys were trained to hold fixation for periods of up to 6 s (Bauer et al. 1980) while visual test stimuli were back-projected at other locations onto a tangent screen. The fixation task involved depressing a lever while waiting for a small light spot to dim, and then releasing the lever within a preset time period after the dim onset (Wurtz 1969). Animals were water-deprived and received one drop of water (0.1 cc) for each successful trial.

The screen was located at a distance of 3.4 m from the monkey, and the fixation target was a yellow light-emitting diode (LED) positioned behind a small aperture. The target appeared as a 3.5′ spot against a black annulus. Visual stimuli appeared beyond the edges of the annulus, but were never able to obscure the fixation spot. Background illumination was 1 fL, and stimuli were between 2 and 5 fL (0.3–0.7 log units above background). The fixation spot was brighter than the stimuli (1.8 log units above background), and the dim decrement (0.14 log units) was made to be just suprathreshold, so the monkey had to be fixating to see it.

Head fixation of the animals during recording sessions was obtained by means of four stainless steel bolts attached chronically to the skull. Eye position was monitored during some initial experiments by means of electrooculogram electrodes embedded in the bone around the eyes (Bond and Ho 1970). Single unit recordings were obtained with glass-coated platinum-iridium electrodes through a cylinder implanted chronically in the skull over the unopened dura (Evarts 1966). Cylinders were positioned so as to permit access to the foveal striate cortex, located between the lateral end of the external calcarine sulcus and the angle formed by the lunate and inferior occipital sulci (Talbot and Marshall 1941). Figure 1 illustrates this region of the brain, both from a surface perspective and in section. In Fig. 1B the junctions between striate and extrastriate cortex are clearly seen at the margins of the occipital operculum, not far from the sulcal lips.

Animals underwent extensive overtraining on the experimental paradigm prior to single unit recording studies in order to assure optimal fixation. Following an initial period of acclimatization to the recording conditions, each monkey achieved a steady working level of greater than 95% correct, receiving in the vicinity of 1,500 rewards (150 cc) per day. Maintenance of animals included regular cleaning of cylinders and headbolt sites, dietary supplements of fresh fruit, and careful monitoring of body weight. Recording sessions lasted 5–6 h per day, 5 or 6 days per week, for more than 1 year in both monkeys, during which time they appeared to remain in excellent health.

The sequence of behavioral events was controlled by a PDP 11/34 computer (Digital Equipment Corporation) using programs written in a combination of Fortran and assembly language (RT11). Single cell responses were amplified, passed through a window discriminator circuit, and then displayed on-line in both raster and histogram form on an oscilloscope. Hard copy was provided by means of an electrostatic printer plotter (Gould 5005).

Receptive fields were mapped with slits of light projected onto the tangent screen. Slit length, width, position and orientation were all continuously adjustable, with position under joystick control. After determining the preferred orientation using a narrow light slit of intermediate length, the receptive field sides (parallel to the preferred orientation) were established by moving

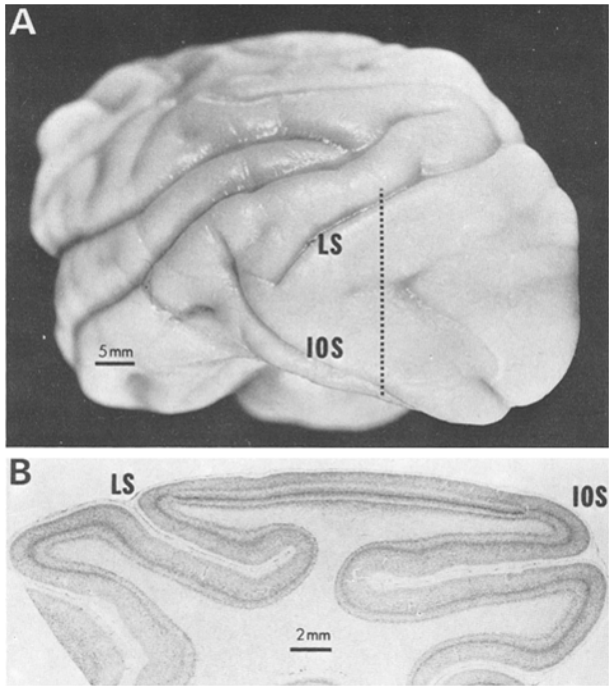

Fig. 1A, B. Foveal striate and extrastriate cortex (left hemisphere) of a rhesus monkey, as viewed on the surface (**A**) and in section (**B**). LS – lunate sulcus. IOS – inferior occipital sulcus. Dashed line in **A** indicates plane of section for **B**

the stimulus slowly back and forth over the active zone. The ends (perpendicular to the preferred orientation) were then determined by making the optimally-oriented stimulus as short as cell responsiveness allowed and moving it from side to side across the field at different elevations. For cells responding only to elongated slits, the receptive field ends were taken to coincide with the preferred length of an optimally positioned slit. In general, receptive field side borders were reproducible to within one minute of arc (1 mm on our screen). Receptive field end borders were reproducible to within several minutes. The hand-mapped receptive field borders were transferred onto acetate sheets attached to the tangent screen. Two investigators were present for mapping, one controlling the stimulus, the other marking the field borders. In some instances receptive field mapping was repeated, using either moving stimuli or stationary flashing stimuli stepped across the field in discrete increments under computer control.

Electrode penetrations were made at 1 mm intervals within each recording cylinder, using a double-eccentric coordinate system (Evarts 1966). The cylinder diameter is 2 cm, with double eccentric coordinates available for a 17 mm diameter circle, giving a total of 223 available sites in a 1 mm grid. Recording sites have been identified on the basis of marking lesions (10 μA of electrode-positive current for 1 min) in some penetrations. Following perfusion, each brain was sectioned in a plane parallel to the angle of the recording electrodes (see Bauer et al. 1980), and then the 32-μm sections stained alternately for Nissl substance and fibers. During the last 5–6 weeks of recording in each monkey, virtually all penetrations were marked. Care was taken not to mark penetrations closer than about 3 mm to one another so as to facilitate later identifications.

The first monkey (Luke) was not refracted, nor was his acuity quantified. The second monkey (Max) was refracted. His values were $-1.00+2.00 \times 80°$ for the right eye and $-1.00+1.50 \times 100°$ for

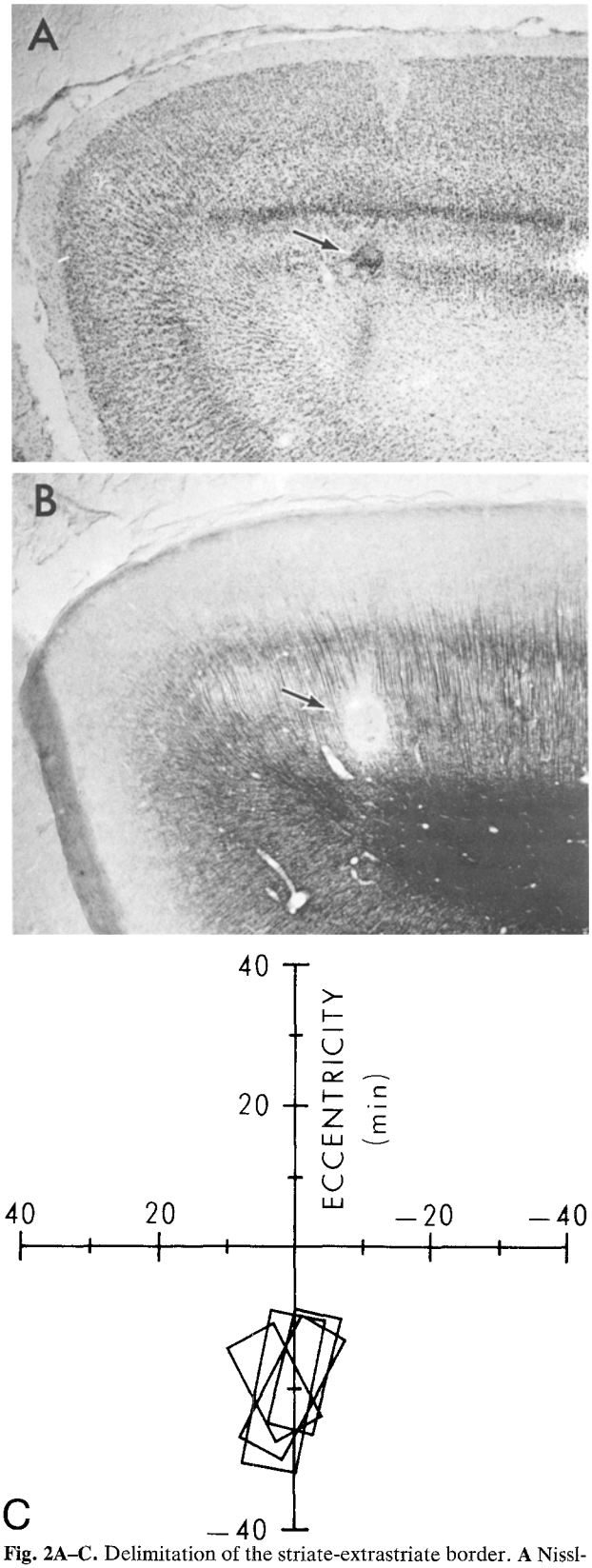

Fig. 2A–C. Delimitation of the striate-extrastriate border. **A** Nissl-stained section showing an electrolytic mark at the deepest of the four recordings illustrated in **C. B** Fiber-stained section of the same mark. **C** Hand-mapped receptive fields of four cells recorded at different depths in a single penetration

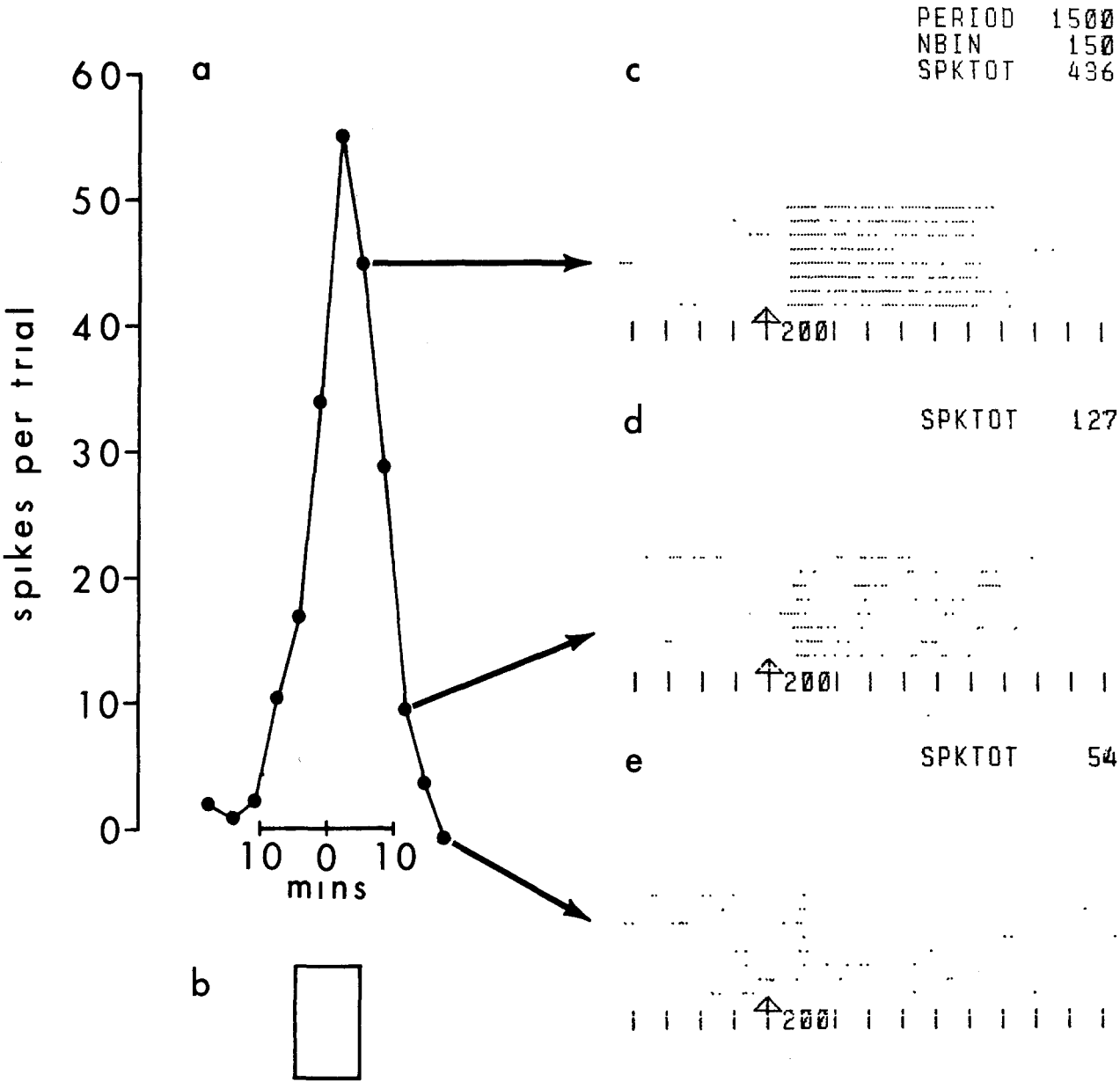

Fig. 3a–e. Receptive field of a cell in foveal striate cortex. Receptive field center at 57 min eccentricity. Computer-mapped field shown in **a.** Handmapped field borders shown in **b.** Horizontal scale applies to both **a** and **b.** Vertical scale indicates average net spikes per trial (response minus spontaneous activity). Preferred stimulus was a light slit 3′×70′, oriented 17° clockwise from vertical. Responses at 3 representative stimulus locations (6′ apart) are displayed as rasters in **c, d,** and **e.** Each raster line corresponds to a single interleaved trial; each dot corresponds to one or more action potentials. The arrows labelled "200" indicate stimulus onset. Time base 100 ms between lines

the left eye. His acuity was tested by means of sinusoidal gratings displayed on an oscilloscope screen according to the procedure of Campbell and Green (1965). The monkey was trained to watch the oscilloscope and release his response bar when the stripes disappeared. Brightness was maintained constant while contrast changed abruptly from 68% to zero after a variable duration fixation period, following our standard behavioral paradigm. Spatial frequency was changed randomly, and the monkey's threshold determined. Three human subjects with normal visual acuity (corrected) were also tested under these conditions. Two had thresholds of 30 cycles/degree, the other 36 cycles/degree. The monkey's thresholds were 19 cycles/degree for vertical and 15 cycles/degree for horizontal. Following application of trial lenses to correct his refraction error, he achieved 19 cycles/degree for both horizontal and vertical. The lenses thus corrected his astigmatism but did not improve his overall performance.

Results

The present report is based on 813 striate cells recorded in 258 penetrations in two rhesus monkeys. Figure 2C illustrates one such penetration, which

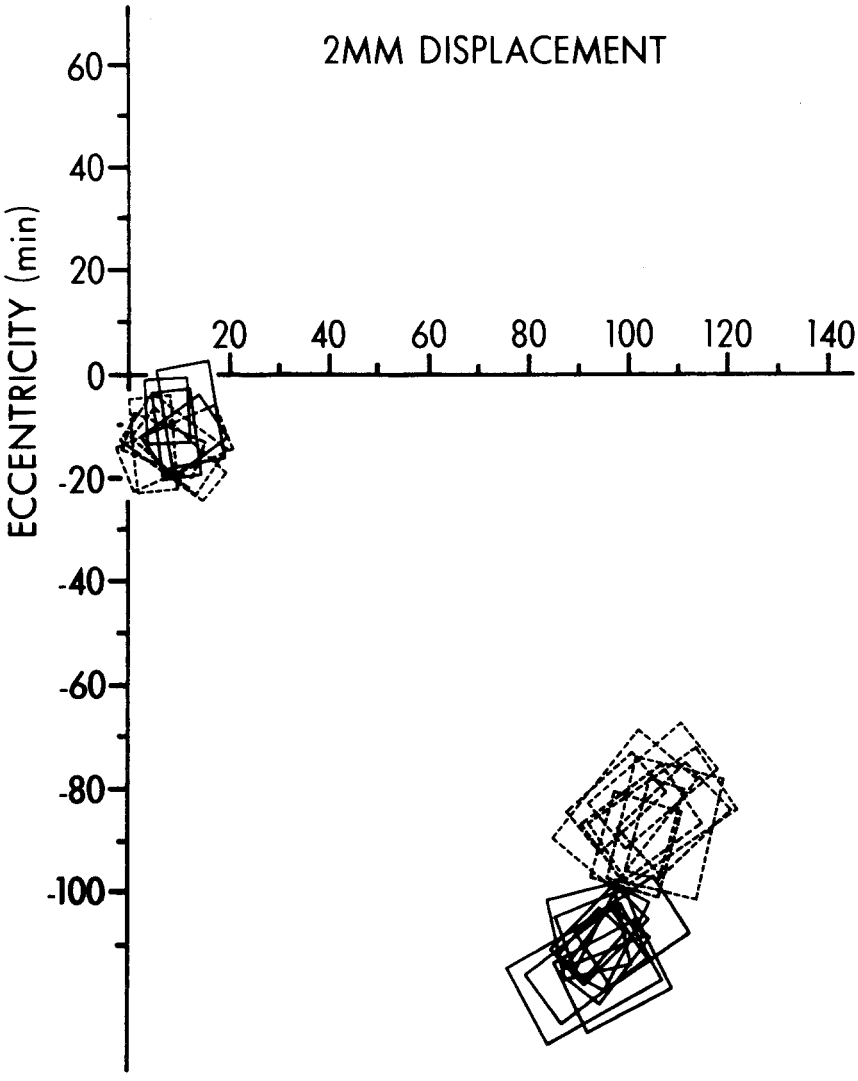

Fig. 4. Overlap of striate receptive fields recorded in pairs of vertical penetrations displaced 2 mm from one another on the cortical surface. For each pair, dashed lines represent receptive fields from one penetration, solid lines represent receptive fields from the other penetration. One pair of penetrations was made in central foveal representation (15′ eccentricity), the other in peripheral foveal representation (110′ eccentricity)

yielded four receptive fields just on the inferior vertical meridian at an eccentricity of about 20 min. Figure 2A and 2B show the recording site of the fourth cell in the deeper layers of striate cortex just inside the border with extrastriate cortex. The four receptive fields shown in Fig. 2C are thus established as striate fields. We feel confident that all cells included in this study were in fact striate cells. Data concerning extrastriate cells will be presented at a later time.

Figure 3 shows the correspondence between a receptive field as mapped by computer (Fig. 3a) and by hand (Fig. 3b). Computer mapping was done by having the stimulus flash on the screen at each of 12 preset positions (at 3′ intervals in this case). The sequence was repeated eight times in an interleaved fashion, thus resulting in a series of 12 rasters of eight lines each. Three such rasters obtained at 6′ intervals are shown in Fig. 3c–e. Note that the responses are stable at each stimulus position. Those in Fig. 3c are consistently strong, those in Fig. 3d are consistently intermediate, and those in Fig. 3e are consistently weak. This response consistency provides some assurance that eye fixation was being maintained to within several minutes of arc during test periods.

Figure 4 illustrates the receptive fields mapped during the course of two pairs of penetrations, the penetrations in each pair being 2 mm apart on the cortical surface. Dashed lines indicate receptive fields obtained from one penetration in each pair, solid lines indicate receptive fields obtained from the other penetration. At eccentricities of 100–120 min the two sets of receptive fields are just nonoverlapping, but at eccentricities of 10–20 min the two sets of receptive fields overlap by perhaps 60–70%. Thus Hubel and Wiesel's (1974) cortical displacement distance of 2–3 mm is not nearly sufficient to yield nonoverlapping receptive fields in central foveal

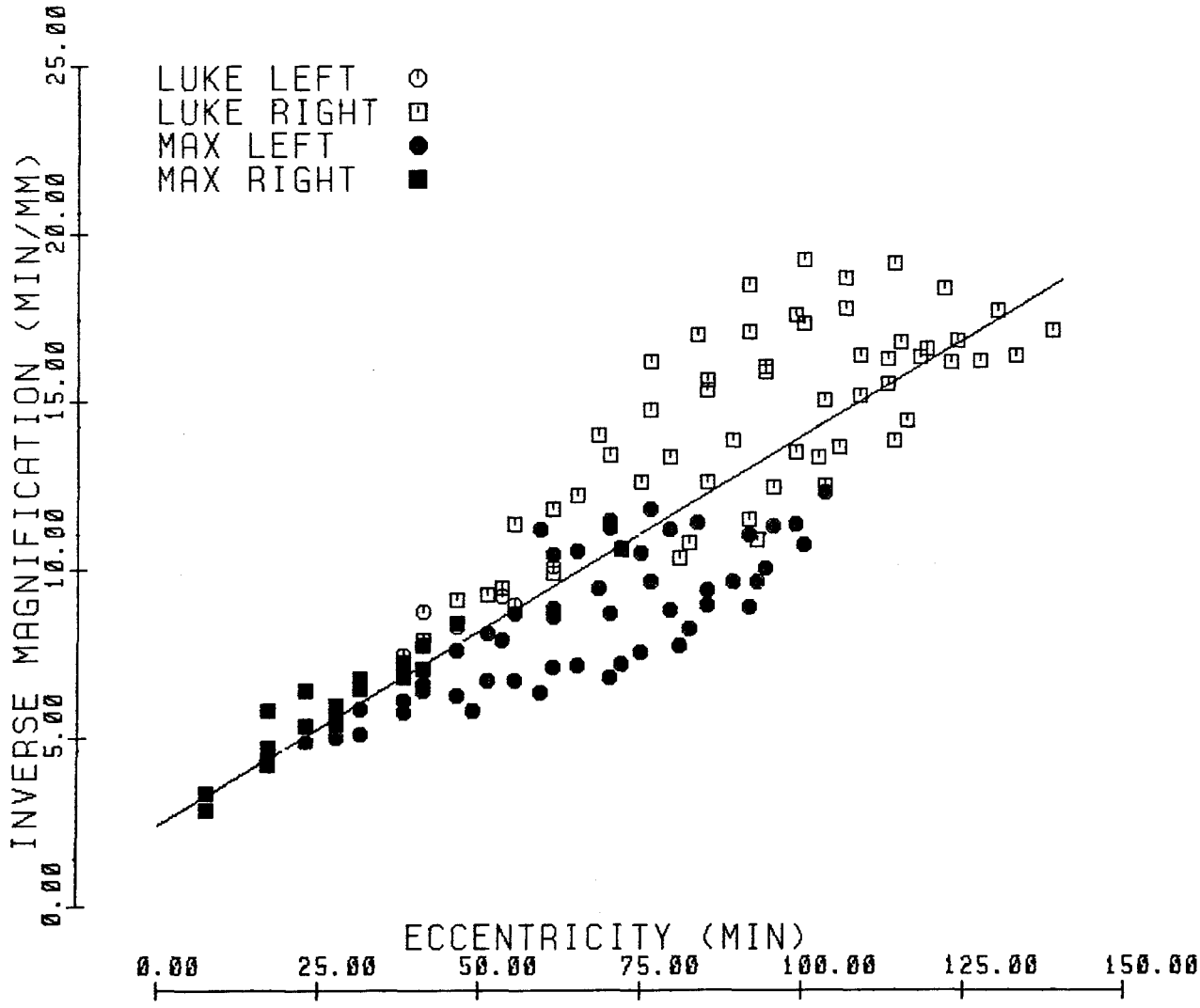

Fig. 5. Inverse magnification in rhesus monkey foveal striate cortex as a function of retinal eccentricity. Data obtained from four hemispheres in two monkeys. Each point is derived from the center eccentricity and size ($\sqrt{\text{area}}$) of a 10′×10′ zone in the retinotopic map for a given hemisphere. The numbers of zones in each map are 56, 52, 20, 6. The equation for the regression line (given in the text) was obtained by a least squares procedure weighing each point equally

cortex, though it is adequate in perifoveal cortex. This is due to the failure of receptive field size to decrease proportionally as magnification increases at low eccentricities.

This issue was examined quantitatively by measuring both inverse magnification and field size as functions of eccentricity within foveal striate cortex. A population of well characterized striate cells with clearly delimited receptive field borders was identified. Each cell then provided six numbers: receptive field length and width, two visual field coordinates, and two recording cylinder coordinates.

To obtain inverse magnification as a function of eccentricity the center of the aggregate receptive field was first determined for each penetration. (About 40% [103/258] of all penetrations included four or more separately recorded cells or cell clusters.) Next the penetrations were grouped according to recording cylinders. The total numbers of penetrations in each of the four cylinders were 85, 69, 60, 44. Each penetration was then plotted as a single point in a scatter plot for that cylinder in visual space using millimeter graph paper (1 mm = 1′). The graph paper was divided into 10′ bins in both the horizontal and vertical directions. An enlarged map of the recording cylinder was labelled with visual field bin locations, and 10′ bin lines were drawn onto the cylinder map. This procedure involved some smoothing of lines, but the large number of data points put major constraints on the location of each line.

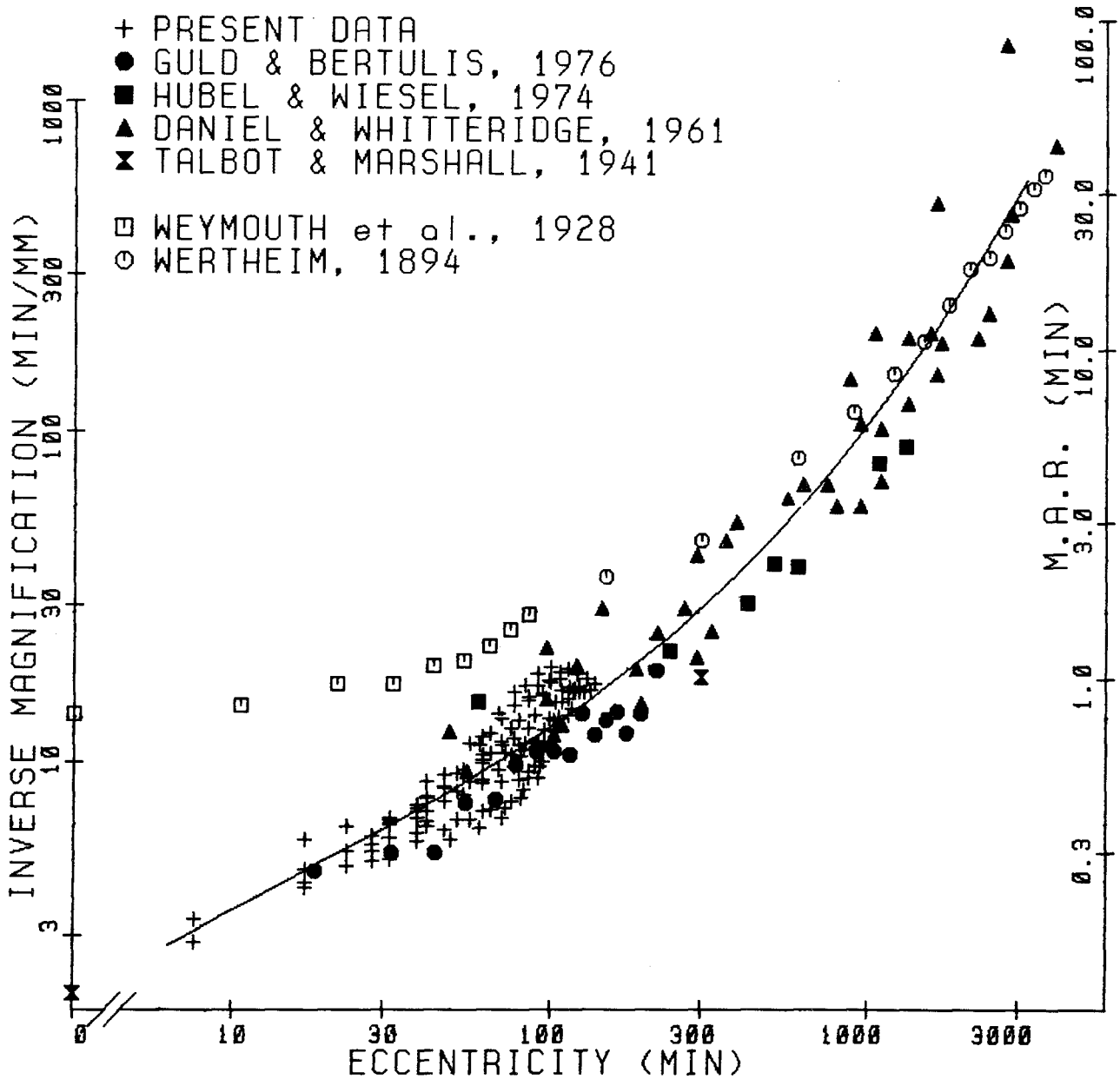

Fig. 6. Inverse magnification in monkey striate cortex as a function of retinal eccentricity from 0° to 50°. Also shown here are minimal angle of resolution data for man (open symbols) plotted on the same coordinate system. The regression line giving log inverse magnification in terms of log eccentricity was obtained by a least squares procedure weighing our points and the previously reported points in ratio 1:3. The result is

$$\log_{10}M^{-1} = 0.8124 + 0.5324x + 0.0648x^2 + 0.0788x^3$$

where $x = \log_{10}E - 1.5$, and E is expressed in minutes

Photographs of the brain surface and histological sections were used to remove from each map regions of high curvature in the vicinity of the external calcarine sulcus (see dimple just to the right of the dashed line in Fig. 1A).

Each map now consisted of a series of distorted 10′ × 10′ squares. The details of these maps will be presented at a later time. For the present study the inverse of the size of each distorted square ($\sqrt{\text{area}}$) has been plotted against its center eccentricity (Fig. 5). The different symbols indicate the recording cylinders from which data points were obtained. In presenting the data in this form we avoid for the present any questions concerning relative magnifications in the upper and lower quadrants and along horizontal and vertical meridia.

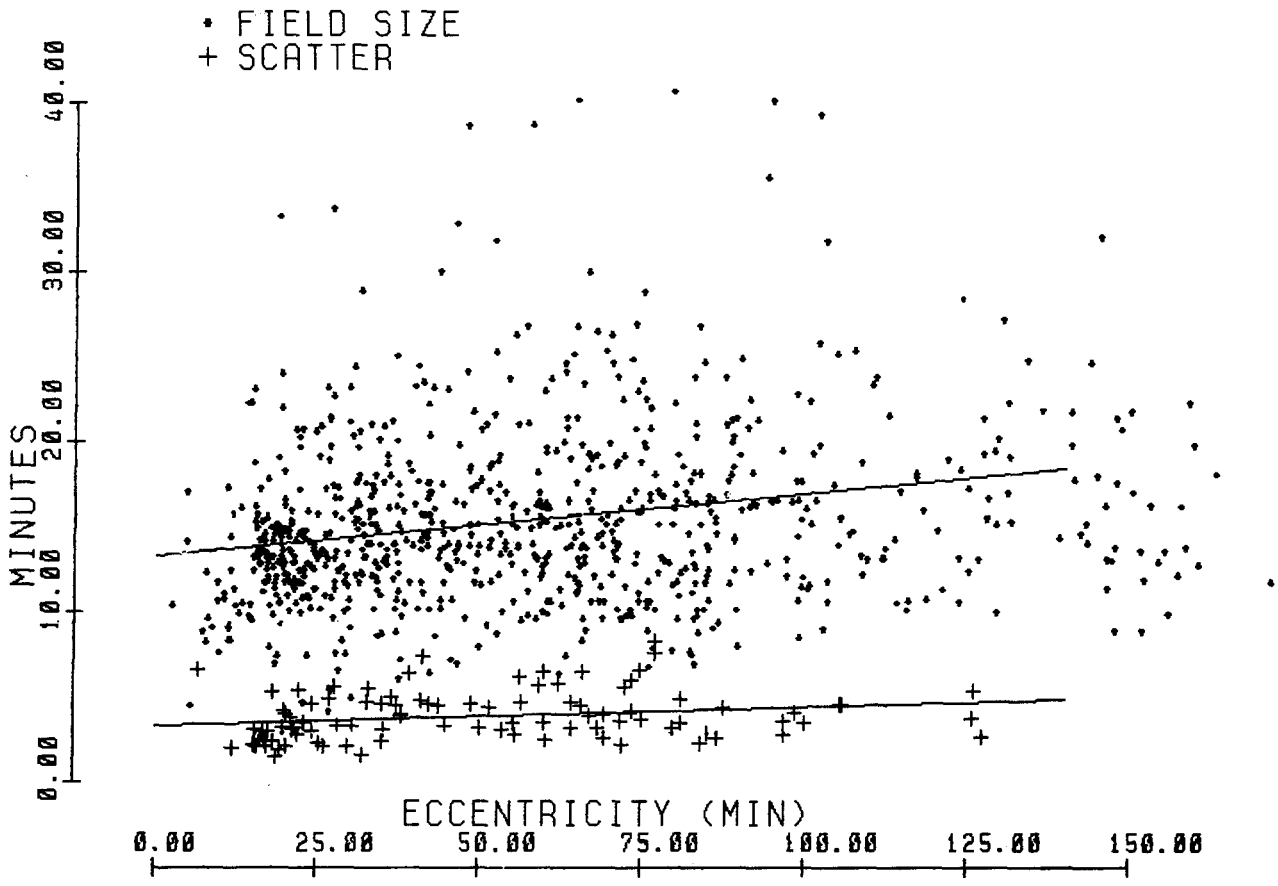

Fig. 7. Receptive field size ($\sqrt{\text{area}}$) and receptive field center scatter (see appendix) in monkey foveal striate cortex as a function of retinal eccentricity. N = 813 for field size, 103 for scatter. The equation for the field size regression line is

f = 13.32 min + 0.037E

The equation for the scatter line is

r = 3.32 min + 0.0116E

The regression line through the data points is described by the equation

M^{-1} = 2.421 min/mm + (0.116/mm)E
(where E is eccentricity in minutes)

This regression line can be compared with Hubel and Freeman's (1977) inverse magnification regression line whose y intercept was 0.109°/mm (6.54 min/mm), and whose slope was 0.0637/mm, or about half of our slope.

To try to get a broader perspective on inverse magnification we have plotted all the currently available data from macaque monkeys in Fig. 6. The data come from five different laboratories, including two points from Talbot and Marshall's (1941) study, and cover a period of 40 years. All data are converted to minutes and plotted on log-log coordinates. The graph also displays data of Wertheim (1894) and Weymouth et al. (1928) on minimal angle of resolution (MAR) as a function of eccentricity, plotted with open symbols.

Considering the diverse sources of the inverse magnification data, it is gratifying to find that the points all fall along the same line, which would not be a straight line on linear coordinates, as Daniel and Whitteridge (1961) recognized. However, in contrast to Daniel and Whitteridge's (1961) claim, the minimal angle of resolution is not related to inverse magnification by a constant of proportionality. Thus, one would not expect to find a fixed acuity distance in striate cortex at all eccentricities. The acuity distance should increase in central fovea. Clearly neither our linear regression line for inverse magnification, nor Hubel and Freeman's (1977) linear regression line provides an adequate fit to all the data.

Field size, the square root of each cell's receptive field area (length × width), is plotted against eccentricity in Fig. 7 for 813 striate cells. Also plotted here is receptive field center scatter for 103 penetrations from which four or more individual cells were recorded. The center scatter data will be discussed later, in relation to Fig. 11.

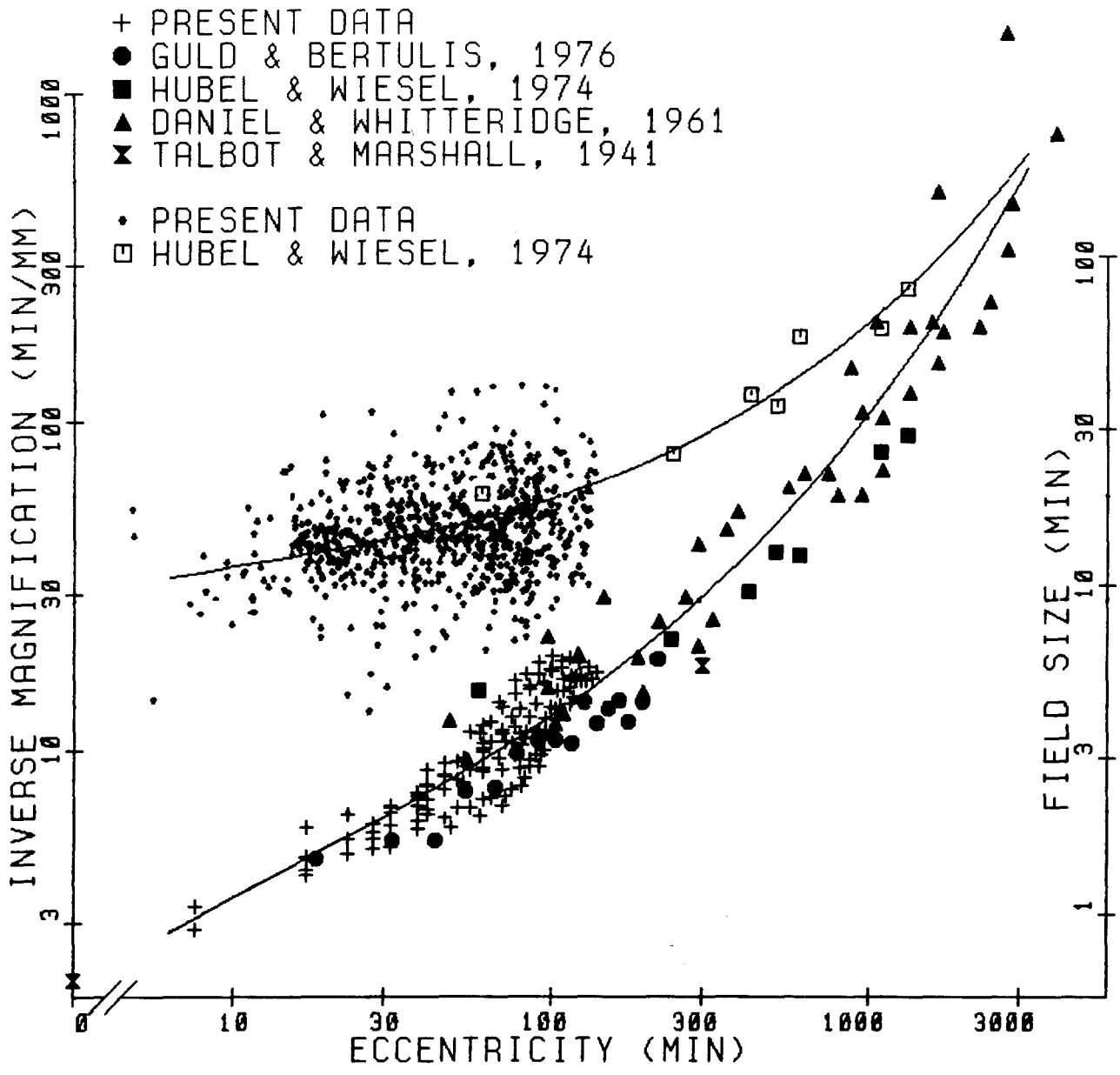

Fig. 8. Field size ($\sqrt{\text{area}}$) and inverse magnification in monkey striate cortex as functions of retinal eccentricity from 0° to 50°. A few dots in the field size scatter plots have been suppressed in order not to obscure one point from Hubel and Wiesel's field size data. The regression line giving log field size in terms of log eccentricity was obtained by a least squares procedure in which our points and Hubel and Wiesel's (1974) points were weighted empirically in ratio 1:50. The result is

$$\log_{10} f = 1.1438 + 0.1920x + 0.0714x^2 + 0.0619x^3$$

where $x = \log_{10} E - 1.5$, and E is expressed in minutes. The line representing M^{-1} is as in Fig. 6

The field size data show considerable vertical scatter at each eccentricity. The occasional cells with relatively large receptive fields (> 30 min) include a distinct group of movement-sensitive neurons (unpubl. data). Scatter within other cortical subgroups (simple vs. complex cells, color vs. noncolor cells, etc.) may be substantially less than the total scatter shown here. We considered the possibility that the smallest receptive fields might be from concentric cells in layer 4C, but in fact only a small percentage of the small field cells lack orientation selectivity. For the present study it seems most straightforward not to subdivide cells in any way, but simply to treat them as a group.

If our receptive field size values are compared with Hubel and Wiesel's (1974) mean field size values (Fig. 8), all the data can be seen to fall along the same curve. This curve is clearly different from the

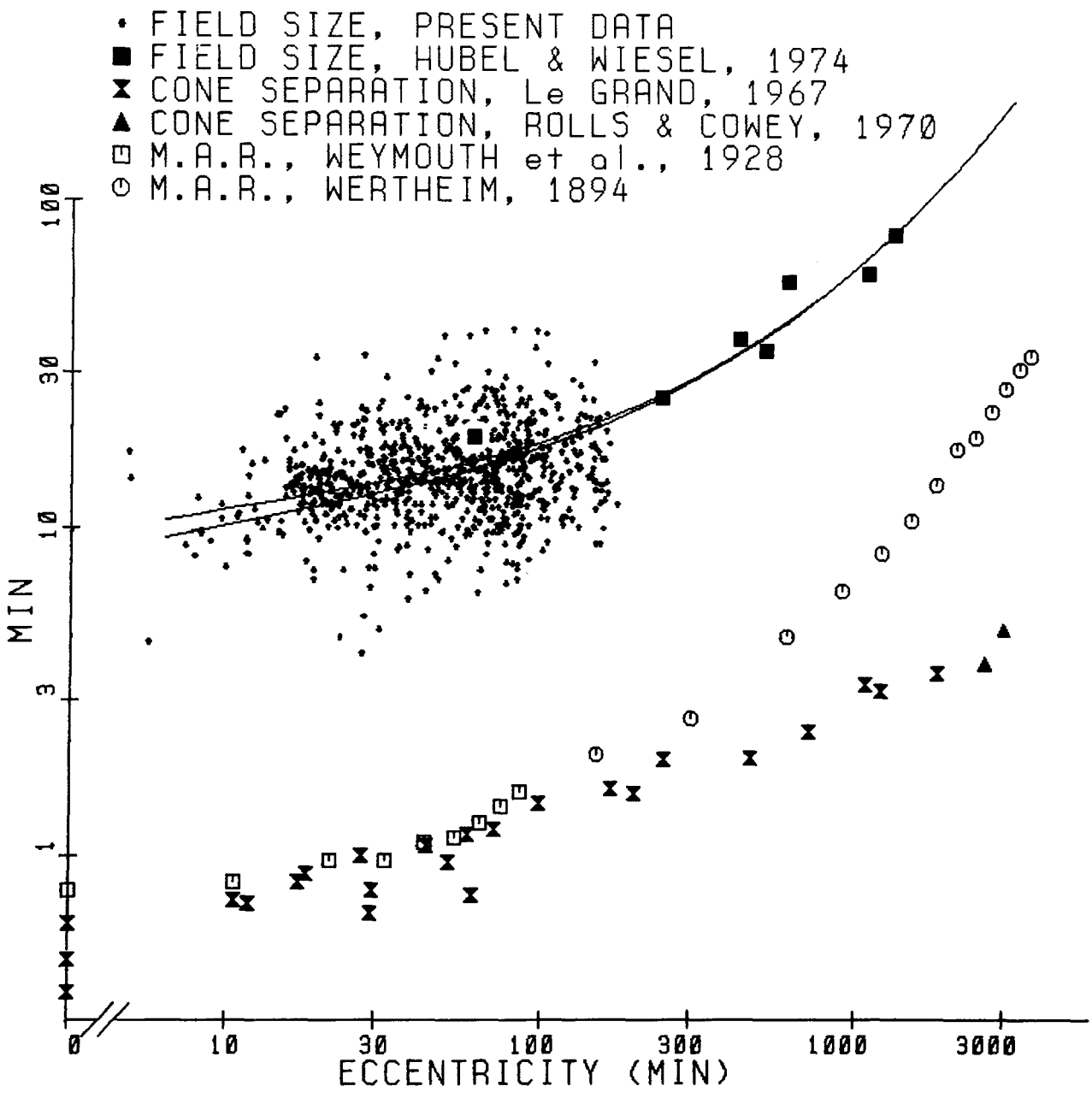

Fig. 9. Field size ($\sqrt{\text{area}}$) in monkey striate cortex compared with cone separation and minimal angle of resolution in man, all plotted as functions of retinal eccentricity from 0° to 50°. Two data points obtained from Rolls and Cowey's (1970) study of cone separation in monkeys are used to extend the human data out to 50°. The lower line through the field size data is obtained by applying a fixed correction of 5 min (see text) to the upper field size curve, which is replotted from Fig. 8

inverse magnification curve. The parallel relationship between log field size and log inverse magnification breaks down in the fovea. Receptive fields do not decrease sufficiently in size to match the change in magnification. Inverse magnification in minutes/mm becomes smaller than field size in minutes at an eccentricity of about 5° (300 min).

Comparison of Figs. 8 and 6 suggests that field size and minimal angle of resolution might be proportional to one another. The two sets of data are plotted together in Fig. 9 and are reasonably parallel on a logarithmic scale, though the field size curve flattens out more at low eccentricity than does the curve for minimal angle of resolution. This discrepancy could be due to the fact that for very small receptive fields the constant error introduced by optical scatter and residual eye movements (an error of perhaps 3–5 min) will have a greater net effect.

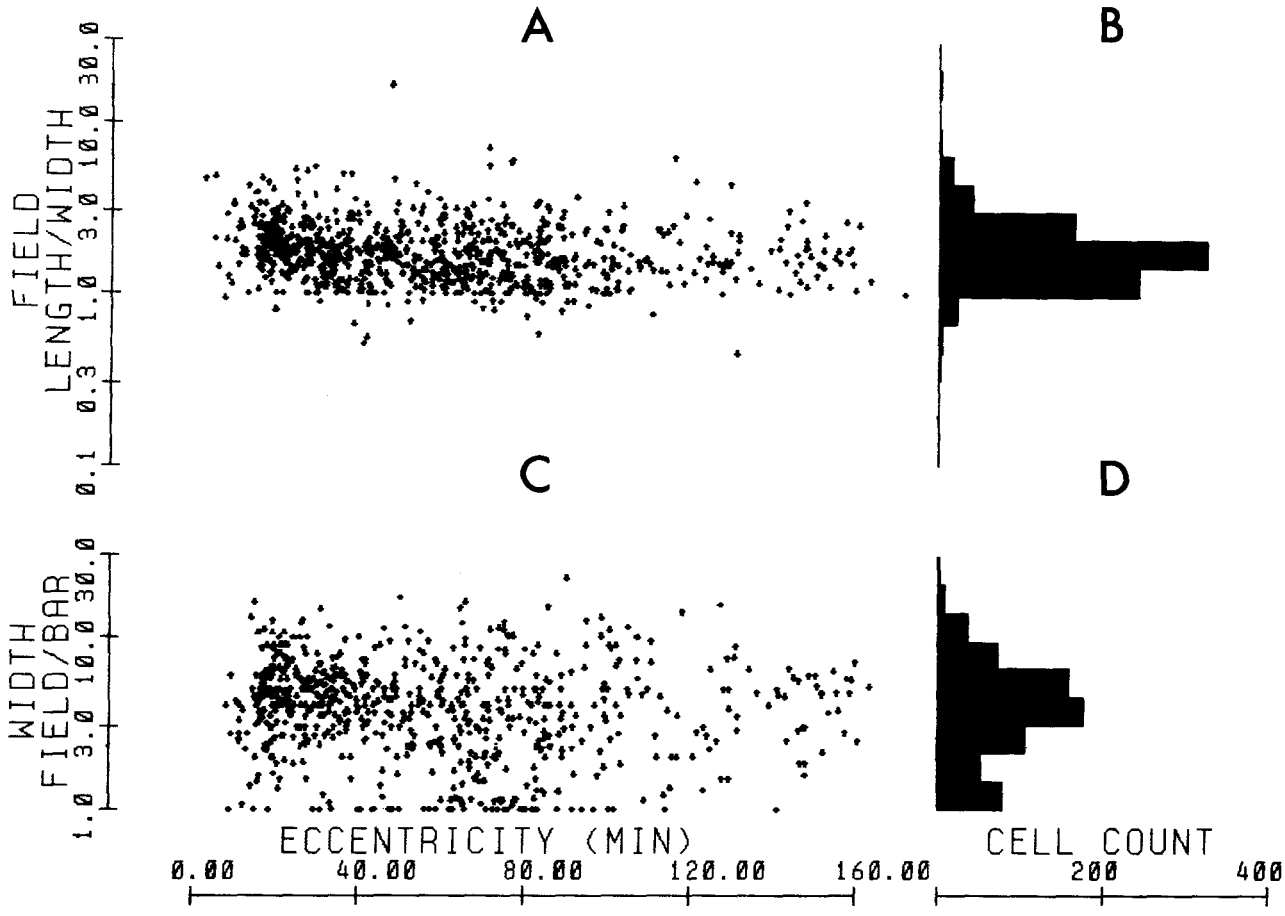

Fig. 10A–D. Ratios of receptive field length to width (**A** and **B**) and of receptive field width to preferred stimulus width (**C** and **D**) in foveal striate cortex as functions of retinal eccentricity. $N = 813$ for **A** and **B**, $N = 640$ for **C** and **D**. Geometric mean for **A** and **B** = 1.71. Geometric mean for **C** and **D** (for all values > 1) = 4.05. Cells for which preferred stimulus width was not determined were excluded from **C** and **D**. Also excluded from **C** and **D** were cells preferring small spots. **A** ratio of 1 in **C** indicates that preferred bar width was equal to or greater than receptive field width

Correction for this error, using an equation of the form

$$R_M^2 = R_E^2 + f^2 \text{ (Fischer 1973)}$$

(where R_M is measured field size, R_E is an error of fixed size, and f is the actual receptive field size) has been carried out here, with $R_E = 5$ min. The slope of the corrected field size curve at low eccentricities is thus brought somewhat closer to that of the minimal angle of resolution curve. It would be useful to have more data at higher eccentricities to see whether the two curves parallel one another outside the foveal region.

Note that both cortical field size and minimal angle of resolution follow the cone separation curve at foveal eccentricities, but deviate sharply from cone separation at 300 min (5°). The relationship between minimal angle of resolution and cone separation is well described by LeGrand (1967), who suggests that minimal angle of resolution may correlate better with ganglion cell density than with cone separation.

The data shown in Fig. 9 suggest a ratio of about 15:1 between foveal cortical field size and cone separation. To examine this relationship more carefully, we have provided additional information about the general shape and internal structure of the receptive fields in Fig. 10. The distribution of receptive field length/width ratios (Fig. 10A) is nearly invariant with eccentricity in foveal striate cortex. The geometric mean of the pooled data is 1.71. A few cells with movement sensitivity have length/width ratios less than one. (Width is always taken as the measure of field size parallel to the preferred orientation.) Very few cells have length/width ratios greater than three. If we take 1.7 as the typical length/width ratio for a cortical cell, then the width is 0.77 of field size, and the ratio of foveal cortical field width to

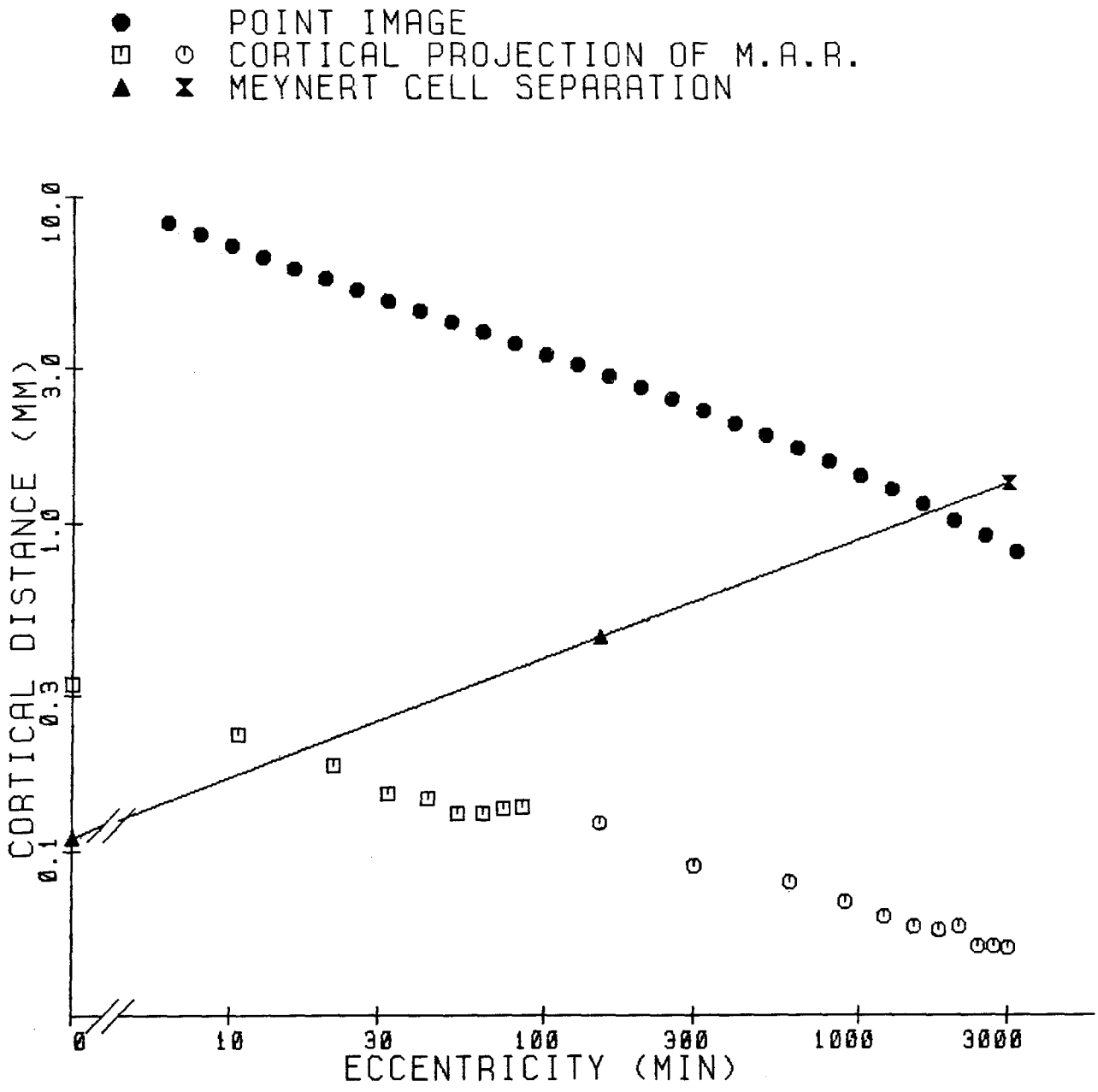

Fig. 11. Point image size in monkey striate cortex as a function of eccentricity. Also plotted are minimal angle of resolution (M A R) for man (see Fig. 6), converted to cortical dimensions, and Meynert cell separation for three eccentricities in the rhesus monkey. ⊡ from Weymouth et al. (1928); ⊙ from Wertheim (1894); ▲ from Chan-Palay et al. (1974); ⧗ from LeGros Clark (1942). Point image is the product of magnification (M) and aggregate field size (F), where

$$F = 4\sqrt{r^2 + s^2}$$

with r a measure of receptive field scatter and s a measure of receptive field size (see text). *r* was taken as 0.314f – 0.86 min by extension of the relationship shown in Fig. 7. The aggregate field includes two standard deviations on either side of the center

cone separation is 11.55:1. A typical foveal striate field is thus 11–12 cones wide. The smallest foveal striate fields are about four to five cones wide.

The distribution of the ratios of receptive field width to preferred stimulus width (Fig. 10B) likewise varies little with eccentricity, having a peak at about 4:1. Combining this information with that obtained from Figs. 9 and 10A, one could say that the preferred stimulus for a foveal striate cell is on the average about two to three cones wide. As the scatter diagram shows, there is a substantial number of cells for which the ratio of receptive field width to stimulus

width is ten or more. A receptive field of average size with field/bar width ratio of 11.5:1 would have a preferred stimulus that was one cone wide. In fact, we found many cells at each eccentricity whose preferred stimulus width was 1 min, which is the approximate size of minimal angle of resolution and cone separation in the fovea. Thus, the information from single cones appears to be preserved in the form of receptive field subunits in striate cortex. The data reported here are consistent with an earlier study by Poggio et al. (1977) reporting spatial frequency tuning peaks in excess of 20 cycles/degree for some foveal striate cells. The individual bars in a 20 cycle/degree grating are 1.5 min wide. It remains to be determined whether an individual cortical cell with a preference for, say, a 1 min wide stimulus, will respond optimally to one, several, or many bars.

Given the fact that the inverse magnification curve has a steeper slope than the field size curve at foveal eccentricities (Fig. 8), it follows that the cortical "point image" (magnification × aggregate field size) should increase at small eccentricities, rather than being invariant with eccentricity as proposed by Hubel and Wiesel (1974). We have calculated aggregate field size according to an argument given in the appendix.

Aggregate field size is here taken to include two standard deviations on either side of the aggregate receptive field center and so will be equal to

$$F = 4\sqrt{r^2 + s^2}$$

where r is a measure of receptive field center scatter, and s is a measure of receptive field size (see below).

Values for r^2 were obtained by direct measurement of receptive field center variance (see appendix) in 103 penetrations containing four or more separately recorded cells or cell clusters. A plot of r vs. eccentricity is shown in Fig. 7. The relationship between the regression lines for handmapped field size (f) and scatter (r) in Fig. 7 is

$$r = 0.314\,f - 0.86 \text{ min}$$

This relationship was extended beyond the upper limit of our measurements (160 min) as an estimate of scatter in terms of field size at all eccentricities.

Values for s^2 were obtained by comparing computer-mapped fields (Fig. 3) with hand-mapped fields from the same cells. For a total of 17 cells examined in this manner it was found that hand-mapped receptive field width was generally about 2× the standard deviation of the computer-mapped receptive field profile. This ratio may reflect our particular criteria for defining receptive field margins. Other laboratories might well come up with a different proportionality constant if they were to repeat this procedure using their own handmapping criteria. We multiplied the hand-mapped receptive field length by the same proportionality constant that we used for width. s^2 was then taken to be $c^2 \cdot \ell \cdot w$, where w is hand-mapped field width, ℓ is hand-mapped field length, and c is the proportionality constant, 0.5 in our case.

Point image size, the product, M · F, where M is magnification, is plotted as a function of eccentricity in Fig. 11. A log-log scale is used so as to permit comparison of point image size with acuity distance at eccentricities ranging from 5 to 3,000 min. At very low eccentricities point image size approaches 10 mm, while acuity distance approaches 0.3 mm. The ratio of the two functions at all eccentricities is about 30:1, which is close to the ratio of Hubel and Wiesel's (1974) nonoverlap distance and Daniel and Whitteridge's (1961) acuity distance, as described earlier. The new finding reported here is that both point image size and acuity distance increase with decreasing eccentricity.

Figure 11 also illustrates an interesting anatomical finding, first reported by LeGros Clark (1942), and more recently confirmed and extended by Chan-Palay et al. (1974). The largest cells in striate cortex, the Meynert cells of layers 5 and 6, are more abundant near the foveal representation than in the periphery. The average linear separation of Meynert cells rises from 110 μm in foveal cortex to 400 μm in perifoveal cortex to 1.33 mm in peripheral cortex. The consequence of this arrangement will be taken up in the discussion.

Discussion

There are two findings contained in this study. The first is that magnification in foveal striate cortex of macaque monkeys achieves values in the range of 30 mm/deg, with inverse magnification approaching 2 min/mm. This was reported 40 years ago by Talbot and Marshall (1941), though subsequent studies have obtained lower values. The second finding is that foveal striate receptive fields are substantially wider than single cones at comparable eccentricities, the mean width of a cortical receptive field measuring 11–12 cone widths, the smallest cortical fields, four to five cone widths.

The slope of the inverse magnification curve is steeper in foveal striate cortex than the slope of the mean receptive field size curve. The consequence of this fact is that foveal receptive fields show much more overlap at any given electrode displacement distance than do more peripheral receptive fields. A

point of light projected onto the fovea is "seen" by many more cortical cells than a point of light projected onto the perifovea, and a perifoveal point is seen by more cortical cells than a peripheral point. This is true despite the fact that cell density in striate cortex is relatively constant irrespective of eccentricity.

Recent measurements indicate the total number of neurons underneath a mm^2 of striate cortical surface in the macaque monkey to be 330,000 (O'Kusky and Colonnier 1980) and 357,200 (Rockel et al. 1980). If we take the diameter of the cortical point image at zero eccentricity to be 10 mm, the area is then about 78 mm^2. If we take 340,000 as the number of striate cells per mm^2, the number of striate cells in a central point image is 2.65×10^7. At eccentricities in the range of 30° (1,800 min) the number of striate cells in a point image becomes 100× smaller, or 2.65×10^5.

The calculations plotted in Fig. 11 show that acuity distance is about 1/30 of point image size. Since point image size as defined here includes two standard deviations on either side of the mean, the acuity distance amounts to 0.133 s.d. If two Gaussians are considered to be unresolvable at separation distances of less than two standard deviations, then the acuity distance is much smaller than what would be required for resolution based on a point image model. The present study suggests it is no longer tenable to consider models of visual acuity involving cone-sized cortical receptive fields. Two-point discrimination at the cortical level is most likely related to size of receptive field subunits rather than size of receptive fields.

Localization in visual space is another matter. Large field cells with subunits would not be expected to be very useful in this regard. Recent work by Westheimer (1979) has suggested that localization in visual space might be achieved by rather different mechanisms than those responsible for resolution. The point spread function in the retina degrades visual images sufficiently to preclude the unique activation of single cones, but a neural mechanism somewhere in the system could theoretically detect the center of a group of activated cones and thus provide localization information even finer than cone separation. A consequence of the inverse magnification data provided in the present study is that Meynert cell separation at eccentricities less than about 20 min (i.e., foveolar eccentricities) is finer than either minimal angle of resolution or cone separation. The potential visual resolution of foveolar Meynert cells is 0.24 min, the projection into visual space of a 100 μm cortical distance where inverse magnification is 2.4 min/mm.

Meynert cells, with cell bodies measuring 30–40 μm across, basal dendrites extending over 800 μm, and apical dendrites extending over 400 μm (Chan-Palay et al. 1974), are by far the largest cells in striate cortex. They apparently sample the more highly processed information available in layers 5 and 6 (over 77% of dendritic spines) and layers 1 and 2 (8–13% of dendritic spines). Recurrent collaterals of Meynert cells could permit lateral inhibition to be exerted upon neighboring Meynert cells. An individual Meynert cell might thus be well suited to provide a precise estimate of total neural activity at a particular cortical locus in comparison to adjacent loci.

A recent study by Bartlett and Doty (1980) suggests that the ability of macaque monkeys to detect phosphenes during microstimulation of striate cortex is related to the proximity of the stimulating electrode to a Meynert cell. It would be worthwhile to see how precisely monkeys can locate phosphenes generated by cortical microstimulation.

Possible Sources of Error

Field Size. Our receptive fields are essentially "minimum response fields" (Barlow et al. 1967). We have not included additional inhibitory zones, subthreshold regions, etc. We have thus if anything underestimated receptive field sizes. This is clear when we compare handmapped fields with computer mapped fields (Fig. 2). It is also evident if one compares our field sizes with those of other investigators (Hubel and Wiesel 1964; Schiller et al. 1976).

Nevertheless, our fields at the lowest eccentricities have undoubtedly been somewhat enlarged by optical factors and residual eye movements. The issue is to try to estimate how much. For humans, Campbell and Gubisch (1968) have shown the line-spread function on the retina to have a half-width at half amplitude of about 0.5 min of arc with a 2.4 mm pupil, and about 1 min of arc with a 6.6 mm pupil. Our monkeys's pupils were not controlled, but we can probably assume they were less than 6 mm. One of our monkeys had a small amount of uncorrected astigmatism. His acuity measured only 15–19 cycles/degree compared with more than 30 cycles/degree for three human subjects, but since corrective lenses did not improve the monkey's acuity (though they did correct his astigmatism) the differences may be behavioral rather than optical. In any case, one would expect optical scatter to reduce the responses of cortical cells rather than to increase receptive field sizes, given the typical preferences of these cells for narrow, properly oriented light bars. Our cells were

in general well driven by their optimal stimulus, as can be seen for one cell in Fig. 3.

Figure 3 also illustrates that residual eye movements probably did not exceed about 3–4′ in these studies. Recordings of eye position with a resolution of 1–2′ of arc using an electromagnetic induction coil have shown that highly trained rhesus monkeys are able to suppress microsaccades in the same way that human subjects can (Steinman et al. 1973). We think that our monkeys may similarly achieve suppression of microsaccades during the extended training they undergo for these experiments. Definitive proof will require recording eye position with a coil (we have recently installed one in our laboratory); but for the present, the stability of cell responses and receptive field maps are suggestive evidence.

If optical and oculomotor factors add a fixed increment of, say, 5 min to our receptive fields, we can correct the field size curve accordingly, and have done so in Fig. 9. Clearly a fixed error of this magnitude would not be sufficient to change any of our major conclusions.

A final issue is binocularity. The receptive fields reported here were mapped with both of the monkey's eyes open and fixating. Some cells undoubtedly had monocular fields. Other cells responding selectively to stimulus locations either in front of or behind the fixation plane (Poggio and Fischer 1977) could have had artifactually widened receptive fields in the fixation plane. However, in our experience such "depth sensitive" cells tend to show weaker responses and smaller fields when tested binocularly than when tested monocularly in the fixation plane.

Magnification. It is important to rule out V2 recording sites. We have closely examined the histology in both monkeys and feel quite sure that no V2 penetrations and few if any individual V2 cells have crept into our totals.

An additional source of error is due to cortical curvature. We did not use penetrations from the vicinity of the external calcarine sulcus in hopes of reducing curvature error. In other parts of foveal striate cortex the surface is rather flat, as reflected in the term "operculum" (a lid) to describe this part of the brain. Nevertheless, there is some residual curvature. We are currently developing computer methods to correct our maps for cortical curvature. The end result of correction for curvature would be, however, even greater magnification rather than less.

Point Image. It may not be valid to extrapolate into the region of Hubel and Wiesel's (1974) data the relationship between mean receptive field center scatter and mean field size established in the region of our data. But since scatter adds a minor contribution to aggregate receptive field size (Fig. 7), the main result shown in Fig. 11 is unlikely to be changed by an improved estimate of scatter at high eccentricities. Similarly, we have used our value (0.5), the ratio between receptive field profile s.d. and hand-mapped field size, with the data of Hubel and Wiesel (1974). The accuracy of our point image curve in the region of their data therefore depends on this assumption.

Acknowledgements. We wish to thank Jeff McCaskey for electronics, Julie Lakatos for illustration, Michelle Stram-Foltin and Steve Bauer for technical assistance, and Susan Wolf for typing. A shorter version of this work was presented in Braunlage, West Germany, in July, 1980, at a satellite symposium of the International Congress of Physiological Sciences.

Appendix

In a single penetration made perpendicular to the cortical surface, the distribution of receptive field center locations may be assumed to be approximately normal. That is, the probability of observing a receptive field center in the differential element of visual space, $dx_c\ dy_c$, is

$$\frac{1}{2\pi r^2} e^{-\frac{(x_c^2 + y_c^2)}{2r^2}} dx_c\ dy_c$$

in the coordinate system with aggregate field center as origin. r^2 may be estimated as

$$2r^2 = \frac{1}{n-1} \sum_i [(x_i - x)^2 + (y_i - y)^2]$$

where (x_i, y_i) is the location of the receptive field center of the i^{th} cell in the penetration (in the coordinate system with the fixation point as origin), $x = \frac{1}{n} \sum_i x_i$, $y = \frac{1}{n} \sum_i y_i$, and n is the number of cells in the penetration.

Let the receptive field size of the i^{th} cell be specified as s_i, where s_i^2 is the variance of the distribution of stimulus position weighted in proportion to response (receptive field profile). Then the aggregate field profile (distribution of stimulus position weighted in proportion to the mean response of all the cells in the penetration) will be approximately

$$\frac{1}{2\pi(r^2 + s^2)} e^{-\frac{(x^2 + y^2)}{2(r^2 + s^2)}}$$

where $s^2 = \frac{1}{n} \sum_i s_i^2$

The variance of the aggregate receptive field profile is then equal to $r^2 + s^2$.

References

Barlow HG, Blakemore C, Pettigrew JD (1967) The neural mechanism of binocular depth discrimination. J Physiol (Lond) 193: 327–342

Bartlett JR, Doty RW (1980) An exploration of the ability of macaques to detect microstimulation of striate cortex. Acta Neurobiol Exp (Warsz) 40: 713–728

Bauer R, Dow BM, Vautin RG (1980) Laminar distribution of preferred orientations in foveal striate cortex of the monkey. Exp Brain Res 41: 54–60

Bond HW, Ho P (1970) Solid miniature silver chloride electrode for chronic implantation. Electroencephalogr Clin Neurophysiol 28: 206–208

Campbell FW, Green DG (1965) Optical and retinal factors affecting visual resolution. J Physiol (Lond) 181: 576–593

Campbell FW, Gubisch RW (1968) Optical quality of the human eye. J Physiol (Lond) 186: 558–578

Chan-Palay V, Palay SL, Billings-Gagliardi SM (1974) Meynert cells in the primate visual cortex. J Neurocytol 3: 631–658

Daniel PM, Whitteridge D (1961) The representation of the visual field in the cerebral cortex in monkeys. J Physiol (Lond) 159: 302–321

Evarts EV (1966) Methods for recording activity of individual neurons in moving animals. In: Rushmer RF (ed) Methods in medical research, vol 11. Year Book, Chicago, pp 241–250

Fischer B (1973) Overlap of receptive field centers and representation of the visual field in the cat's optic tract. Vision Res 13: 2113–2120

Grether WF (1941) A comparison of visual acuity in the rhesus monkey and man. J Comp Physiol Psychol 31: 23–33

Guld C, Bertulis A (1976) Representation of fovea in the striate cortex of vervet monkey, *cercopithecus aethiops pygerythrus*. Vision Res 16: 629–631

Hubel DH, Freeman DC (1977) Projection into the visual field of ocular dominance columns in macaque monkey. Brain Res 122: 336–343

Hubel DH, Wiesel TN (1974) Uniformity of monkey striate cortex. A parallel relationship between field size, scatter, and magnification factor. J Comp Neurol 158: 295–306

Hubel DH, Wiesel TN (1977) Functional architecture of macaque monkey visual cortex. Proc R Soc Lond [Biol] 198: 1–59

LeGrand Y (1967) Form and space vision (translated by Millodot M, Heath GG) Indiana University Press, Bloomington

LeGros Clark WE (1942) The cells of Meynert in the visual cortex of the monkey. J Anat 76: 369–376

McIlwain JT (1976) Large receptive fields and spatial transformations in the visual system. Int Rev Physiol 10: 223–248

O'Kusky J, Colonnier M (1980) The number of neurons, glial cells and synapses in the striate cortex of macaque monkey. A stereological analysis. Neurosci Abstr 6: 578

Poggio GF, Fischer B (1977) Binocular interaction and depth sensitivity in striate and prestriate cortex of behaving rhesus monkey. Neurophysiol 40: 1392–1405

Poggio GF, Doty RW, Jr, Talbot WH (1977) Foveal striate cortex of behaving monkey: single neuron responses to square-wave gratings during fixation of gaze. J Neurophysiol 40: 1369–1391

Polyak S (1957) The vertebrate visual system. University of Chicago Press, Chicago

Rockel AJ, Hiorns RW, Powell TPS (1980) The basic uniformity in structure of the neocortex. Brain 103: 221–244

Rolls ET, Cowey A (1970) Topography of the retina and striate cortex and its relationship to visual acuity in rhesus monkeys and squirrel monkeys. Exp Brain Res 10: 298–310

Schiller PH, Finlay BL, Volman SF (1976) Quantitative studies of single cell properties in monkey striate cortex. I. Spatiotemporal organization of receptive fields. J Neurophysiol 39: 1288–1319

Steinman RM, Haddad GM, Skavenski AA, Wyman D (1973) Miniature eye movement. Science 181: 810–819

Talbot SA, Marshall WH (1941) Physiological studies on neural mechanisms of visual localization and discrimination. Am J Ophthalmol 24: 1255–1263

Wertheim T (1894) Über die indirekte Sehschärfe. Z Psychol Physiol Sinnesorg 7: 172–189

Westheimer G (1979) The spatial sense of the eye. Invest Ophthalmol Vis Sci 18: 893–912

Weymouth FW, Hines DC, Acres LH, Raaf JE, Wheeler MC (1928) Visual acuity within the area centralis and its relation to eye movements and fixation. Am J Ophthalmol 11: 947–960

Wurtz RH (1969) Visual receptive fields of striate cortex neurons in awake monkeys. J Neurophysiol 32: 727–742

Received October 15, 1980